ELECTRODEPOSITION OF CADMIUM ON N-TYPE SILICON SINGLE CRYSTALS OF DIFFERENT SURFACE ORIENTATIONS

BOUBIÉ GUEL

ABSTRACT

The mechanisms related to the initial stages of the nucleation and growth mechanism of cadmium on (100) and (111) n-type silicon have been studied as a function of different potential steps. Within appropriate potential ranges the initial deposition kinetics corresponds to a model including progressive nucleation and diffusion controlled cluster growth. Nucleation rate and the number of atoms in the critical nucleus are determined from the analysis of current transients at different overpotentials. Values of N_{crit} are 16 ± 1 (-16 mV ≥ η ≥ -19 mV) and 7 ± 1 (-14 mV ≥ η ≥ -18 mV) for n-Si(100) and n-Si(111) respectively.

KEYWORDS: Electrodeposition; n-Si(111); n-Si(100); Nucleation and growth mechanism.

1. INTRODUCTION

The process of electrolytic deposition of metals on metal and semiconductor substrates is gaining considerable scientific interest because it is a relatively low energy process compared with other methods such as conventional UHV deposition. From a technological standpoint, metal deposition in form of thin films on semiconductor surface is important in the fabrication of integrated circuits (Brillsoin, 1982) and solar energy conversion (Allongue, 1992).

In recent years, various metals have been successfully electrodeposited on metal and semiconductor substrates. A comprehensive review of metal electrodeposition can be found in (Budesvski, et al.). The interest in thin films of cadmium is increasing considerably due to its use in the electrodeposition of CdX (X = S, Se, Te, O) compound thin films or nanostructures (Hodes, et al., 1992; Hodes, 1993; Golan, et al., 1994; Gómez, et al., 2004; Gómez, et al., 2005; Djenizian, et al., 2001; Ortega, et al., 2000). Since these thin films or nanostructures are grown from plating bath containing Cd^{2+} ions, it is of great interest to understand the fundamentals of cadmium electrodeposition. Although many works have been carried out on the cadmium electrodeposition on various substrates such as Bi, Sn and Pb (references cited in Maupai, et al., 2003), Ag (Bort, et al., 1983), Au (Maupai, et al., 2003; Vidu, et al., 2000), Cu (Hümann, et al., 2003), or GaAs (Khader, et al., 1999), only a limited number of fundamental studies of Cd electrodeposition have been carried out on silicon single crystals. In previous work (Krumm, et al., 2000) we examined Cd electrodeposition, from a solution containing 5 x 10^{-3} M Cd^{2+} ions, on n- Si(111) (1-5 Ωcm resistivity and 0° misorientation). It was shown that within appropriate potential ranges the initial deposition kinetics corresponded to a model including progressive nucleation on active sites and diffusion controlled cluster growth. Nucleation rate and the number of atoms N_{crit} in the critical nucleus were determined from the analysis of current transients at different overpotentials. A value of 6 was derived for N_{crit} with an accuracy of ± 1 in the overpotential range -15 ≥ η ≥ -21 mV (Krumm, et al., 2000).

Generally, the technique used for deposition is as follows: the working electrode is prepolarized with respect to the reference in solution at a selected underpotential ΔE_i, where no current flows. At t = 0, the potential step raises the Fermi level to a potential corresponding to an overpotential η = $(E - E_{Me^{z+}/Me}) < 0$. The main electrocrystallization parameters besides those relative to the substrate are ΔE_i, η, the time of deposition and the solution composition (pH,

concentration, etc.). The purpose of this paper is a comparative study of the initial stages of nucleation and growth of electrodeposited Cd on n-type silicon single crystals of different surface orientations. This work confirms the strong orientation dependence of the electrochemical process and is therefore of fundamental interest in electrochemical phase formation, phase transition and dissolution processes which play an important role in the preparative aspect of electrochemical nanotechnology.

2. METHODS

The investigations were carried out in the systems[•]: n-Si(*hkl*) / 5 x 10^{-3} M $CdSO_4$ + 0.5 M Na_2SO_4 + 5 x 10^{-3} M H_2SO_4; pH = 2.5, T = 298 K, where (*hkl*) = (111), (100).

Silicon working electrodes were made from n-type silicon wafers of different surface orientations: 1) (100) orientation, phosphorus-doped, 20-40 Ωcm resistivity, MEMC Electronic Materials, Germany; 2) (111) orientation, phosphorus-doped, 40-60 Ωcm resistivity, Wacker Siltronic AG, Germany. The geometrical surface area of the substrates was approximately 1 cm^2.

The Si(*hkl*) substrates were subsequently cleaned in trichloroethylen, acetone and methanol and etched for 1 min in 2% HF solution and 6 min in deaerated 40% NH_4F solution. The substrates were then mounted into a Teflon holder with their polished side in contact with the electrolyte. Ohmic contact was established on the back of the Si samples with a Ga/In eutectic.

The electrolytes were prepared from suprapure chemicals and fourfold-distilled water and deaerated by purified nitrogen prior to and during each experiment.

Conventional electrochemical measurements were performed in a three-electrode electrochemical cell with a Pt-counter electrode and a small Pt sphere covered with electrochemically deposited Cd used as the reference electrode and placed at a distance of 1-2 mm near the silicon-working electrode in order to ensure negligible ohmic drop in all experiments. All electrode potentials are referred to the equilibrium potential of the 3D Cd bulk phase $E_{3D\ Cd}$.

3. RESULTS AND DISCUSSION

Deposition on n-Si(100), phosphorus-doped, 20-40 Ωcm resistivity.

Figure 1 shows typical cyclic voltammograms of Cd deposition obtained at T = 298 K with |dE/dt| = 1 mVs^{-1} in the system n-Si(100) / 0.005 M Cd^{2+}. In the system under investigation, no peak can be found in the UPD (underpotential

Boubié Guel, Laboratoire de Chimie-Physique et d'Electrochimie, UFR-SEA, Université de Ouagadougou, 03 BP 7021 Ouagadougou 03 Burkina Faso.

deposition) range indicating a weak interaction (weak adhesion) of cadmium with n-Si(100). Current loop in the OPD (overpotential deposition) range, typical of a nucleation-growth process at electrode surfaces, is observed. Actually, in such systems (semiconductor substrates) where the binding energy of Me^* adatoms on the substrate S, i.e. ($\Psi_{Me_{ads} - S}$), is lower than that of Me adatoms on the native substrate, i.e. ($\Psi_{Me_{ads} - Me}$), the 3D Me phase is formed in the OPD range on top of an unmodified substrate following a Volmer-Weber growth mechanism (Pötzschke, et al., 1999). Further, anodic peak corresponding to the metal stripping can be seen in the positive voltammetric scan indicating that deposition and dissolution of Cd are reversible in this system.

Figure 2a shows current transients for Cd deposition on n-Si(100) 20-40 Ωcm resistivity. The deposition rate increases with overpotential η. The analysis of the transients was restricted only to their initial part in order to exclude overlapping effects of growing 3D Cd clusters and/or diffusion zones. The transient current density under these conditions is defined as i_{free}. Figure 2b shows the initial parts of the transients in a $(i_{free})^{2/3}$ vs. t plot. All the linear relationships were obtained with coefficients of determination R^2 greater than 0.9025. This indicates the goodness of fit of the data to a straight line (Billo, 1997). The obtained linear relationships correspond to a nucleation and growth model including progressive nucleation and hemispherical diffusion to the growing 3D Cd clusters, where i_{free} is given by (Budesvski, et al., 1996)
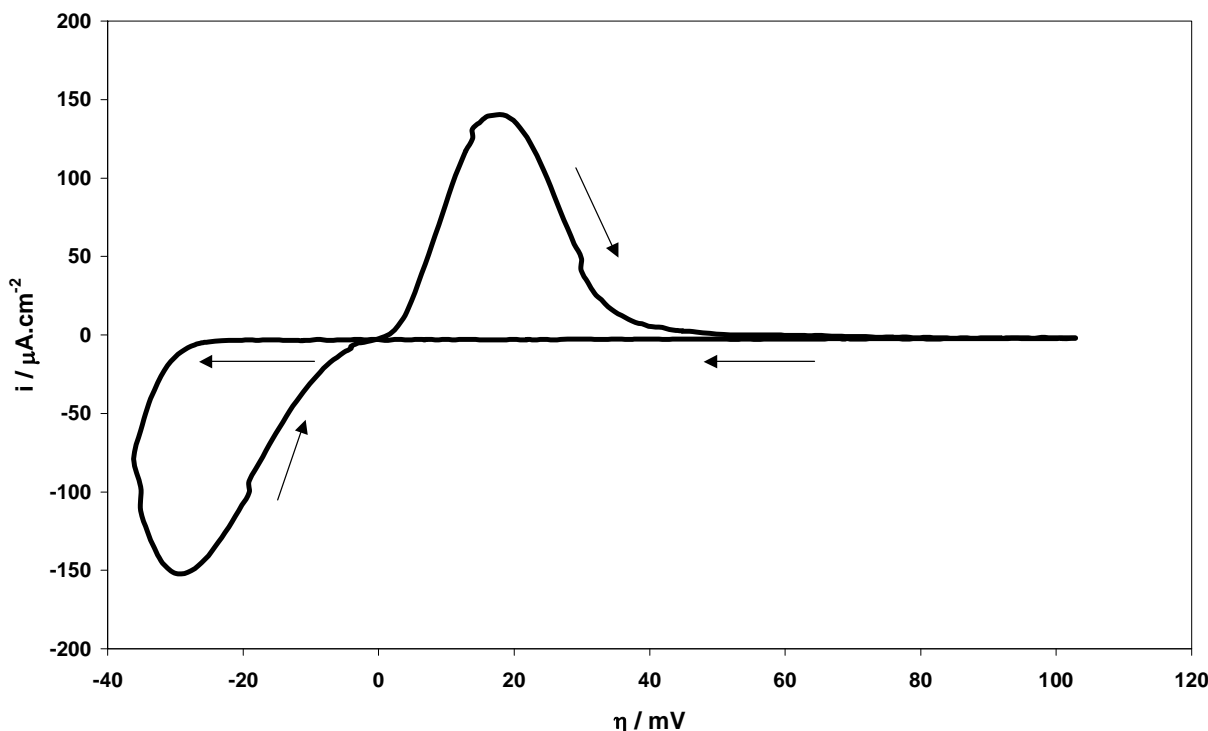
$$i_{free} = -zF \frac{2}{3} \pi \, V_m^{1/2} \, J(2DC_{Cd}^{2+})^{3/2} [1-\exp(\frac{zF\eta}{RT})]^{3/2} (t-t_0)^{3/2} \qquad (1)$$

Figure 1: Cyclic voltammogram for Cd deposition and dissolution in the system n-Si(100): 20-40 ohm.cm / 5 x 10^{-3} M CdSO$_4$ + 0.5 M Na$_2$SO$_4$ + 5 x 10^{-3} M H$_2$SO$_4$; pH = 2.5, T = 298 K, $|dE/dt|$ = 1 mVs^{-1}.

where V_m represents the molar volume of the bulk metal Cd, F the Faraday constant, D the diffusion coefficient of Cd^{2+} ions, C_{Cd}^{2+} the metal ion bulk concentration, and t_0 the induction period. The nucleation rate J in equation (1) is defined by (Budesvski, et al., 1996)

$$J(\eta) = A\exp[-\frac{\Delta G_{crit}(\eta)}{kT}] \qquad (2)$$

where $\Delta G_{crit}(\eta)$ is the Gibbs free energy for the formation of a critical cluster containing N_{crit} atoms. The pre-exponential factor A includes the number of active nucleation sites as well as the attachment frequency of single atoms to nucleus. The nucleation rates J were derived from the slopes of these plots using equation (1) with V_m = 13,0074 cm^3 mol^{-1} and D = 8,64.10^{-6} cm^2 s^{-1} (Lobo, 1989).
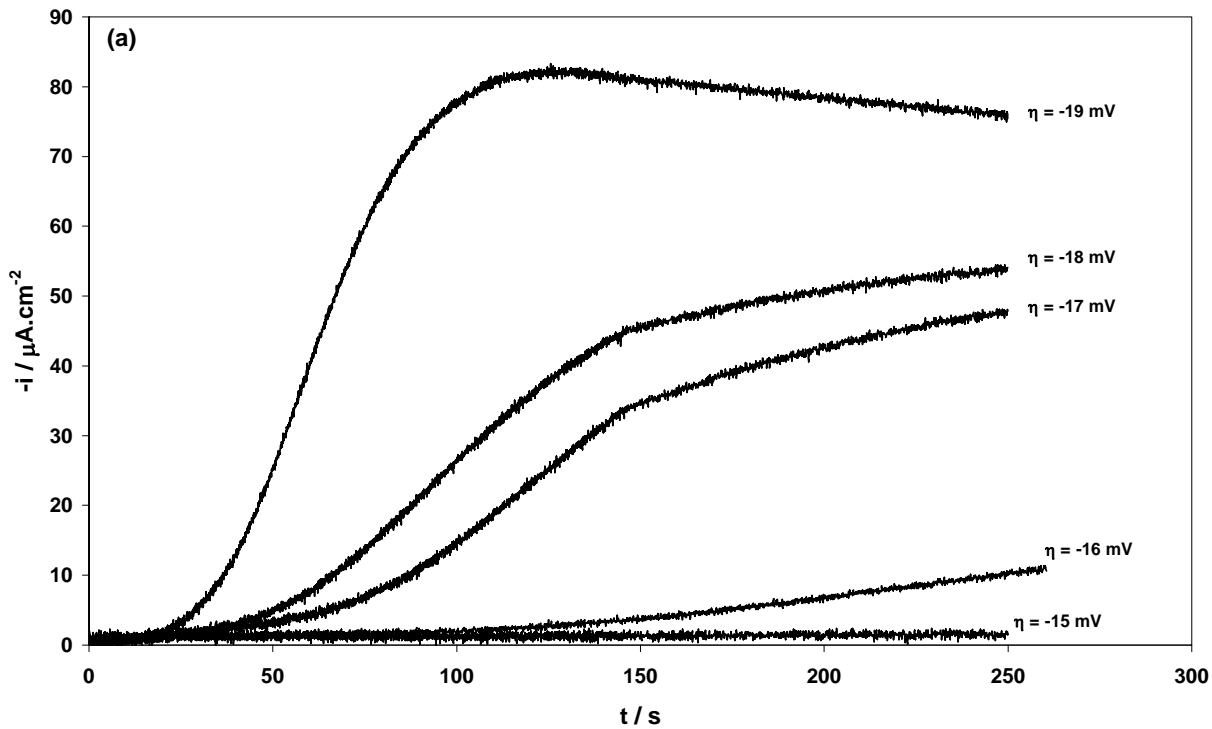
Figure 2a: Experimental current-time transients for Cd OPD at different overpotentials η in the system n-Si(100): 20-40 ohm.cm / 5 x 10^{-3} M $CdSO_4$ + 0.5 M Na_2SO_4 + 5 x 10^{-3} M H_2SO_4; pH = 2.5, T = 298 K. Initial potential $\Delta E_i = E - E_{Cd^{2+}/Cd} = 0$ mV.
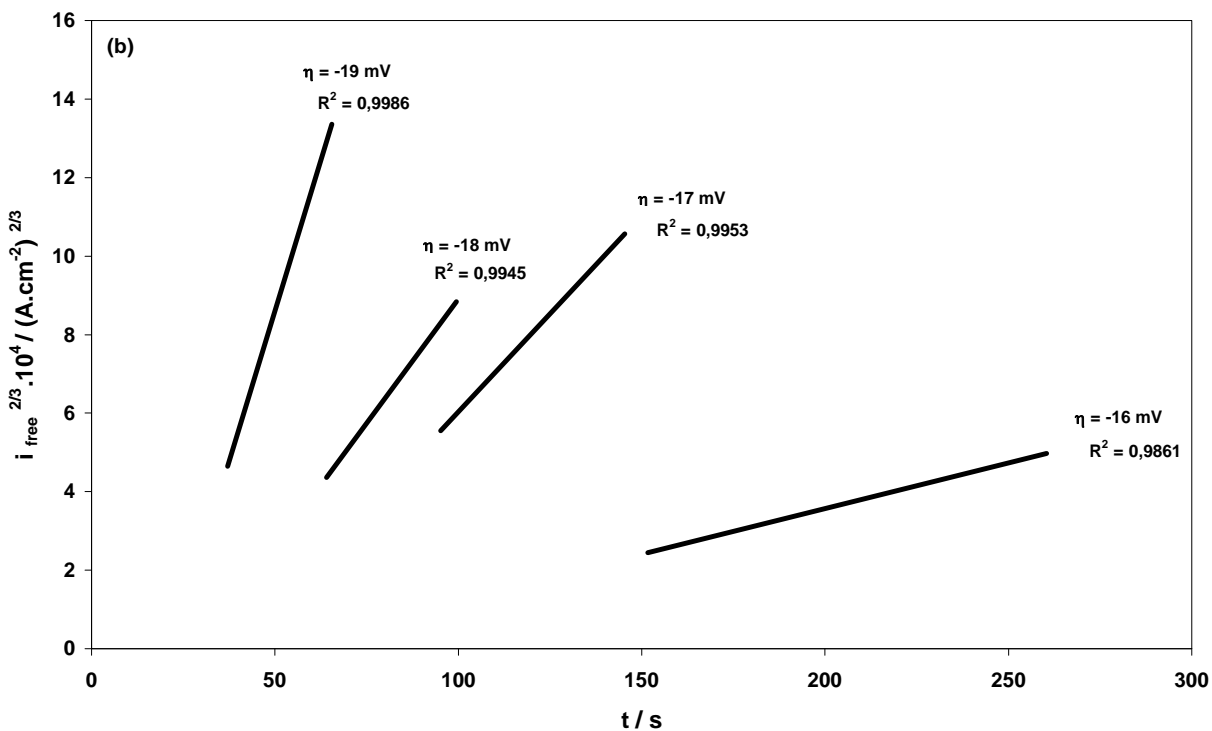

Figure 2b: $i_{free}^{2/3}$ vs. t plot of the initial parts of the transients shown in Figure 2a.

Figure 3 shows the nucleation rate J as a function of the overpotential $|\eta|$ for the system under investigation. Linear ln J- $|\eta|$ dependence is obtained in this overpotential range with a coefficient of determination R^2 greater than 0.9025 and in agreement with equation (2). The number of atoms N_{crit} in the critical cluster can be determined using equation (3)

$$N_{crit} = \frac{RT}{zF} \frac{d\ln J}{d|\eta|} \qquad (3)$$

In this equation the weak overpotential dependence of the pre-exponential, A, in equation (2) is neglected because it affects N_{crit} only by less than 1 atom. From the slope of the linear ln J - $|\eta|$ dependence shown in Figure 3 a value of N_{crit} = 16 ± 1 atoms was derived for the substrate in the overpotential range -16 mV ≥ η ≥ -19 mV using equation (3). The small number of atoms in the critical cluster indicates that the nucleation process has to be described by the so-called atomistic model (Budesvski, et al., 1996).
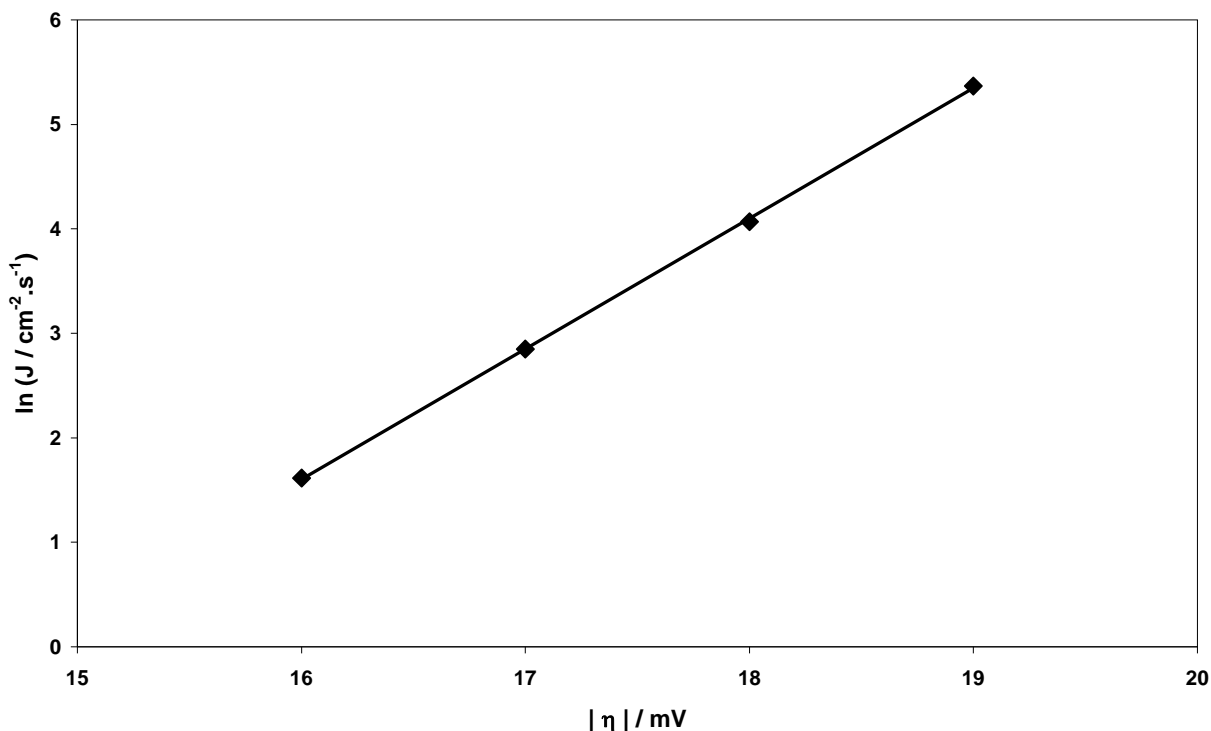
Figure 3: Nucleation rate J as a function of the overpotential   . System n-Si(100): 20-40 ohm.cm / 5 x 10^{-3} M CdSO$_4$ + 0.5 M Na$_2$SO$_4$ + 5 x 10^{-3} M H$_2$SO$_4$; pH = 2.5, T = 298 K.
Coefficient of determination of the straight line: R^2 = 0.9998. N$_{crit}$ = 16 ± 1 atoms.

Deposition on n-Si(111), phosphorus-doped, 40-60 Ωcm resistivity.

Figure 4 shows a cyclic voltammogram of the system n-Si(111): 40-60 *Ωcm* resistivity/ 0.005 M Cd^{2+}. The electrochemical behavior is the same as for Cd deposition on n-Si(100) (described above) and on n-Si(111): 1-5 *Ωcm* resistivity, 0° misorientation (Krumm, et al., 2000). The same analysis can also be applied in this case.

Typical current transients for nucleation and growth of Cd on n-Si(111): 40-60 *Ωcm* resistivity are shown in Figure 5a. The obtained linear i$_{free}^{2/3}$ vs. t relationships for the initial parts of the transients (Figure 5b, coefficient of determination R^2 greater than 0.9025) correspond to a progressive nucleation and diffusion controlled cluster growth described by
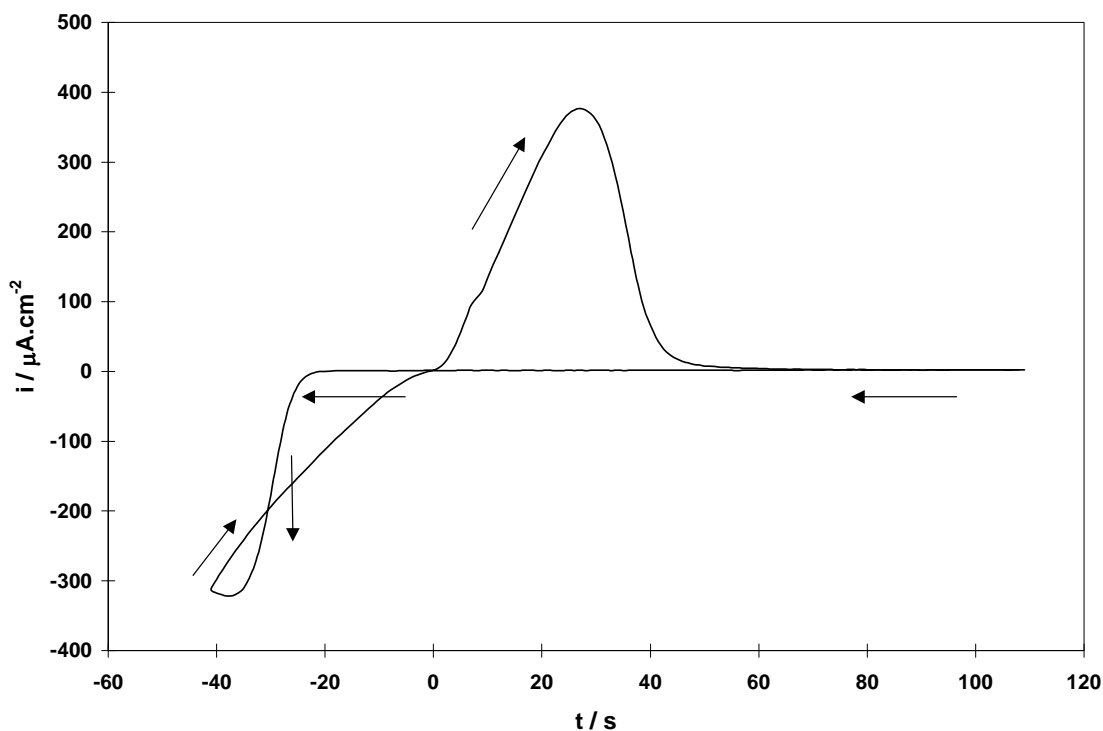

Figure 4: Cyclic voltammogram for Cd deposition and dissolution in the system n-Si(111): 40-60 ohm.cm / 5 x 10^{-3} M CdSO$_4$ + 0.5 M Na$_2$SO$_4$ + 5 x 10^{-3} M H$_2$SO$_4$; pH = 2.5, T = 298 K, │dE/dt│ = 1 mVs^{-1} .

equation (1). The nucleation rates J at different overpotentials were derived from the slopes of the $i_{free}^{2/3}$ vs. t plots in Figure 5b and equation (1). Applying equation (3), a value of $N_{crit} = 7 \pm 1$ was estimated from experimental data denoting the linear ln J- | η | dependence in the overpotential range –14 mV ≥ η ≥ -18 mV (Figure 6). Within experimental errors, these results are similar to those obtained for cadmium deposition on n-Si(111): 1-5 Ωcm resistivity, 0° misorientation and indicate that: a) the miscut angle of (111) surfaces and the resistivity do not have a great influence on the value of N_{crit} in the critical cluster; b) the so-called atomistic approach has to be applied to describe the nucleation processes in these systems (Budesvski, et al., 1996). Moreover, such a N_{crit}-value is not specific to n-type (111) Si wafers. A N_{crit}-value ranging between 7 and 8 was found in the case of cadmium deposition on graphic HOPG (0001) substrate (Guel, 2007, University of Ouagadougou). The difference in the N_{crit}-value between n-Si(100) and n-Si(111) samples can be related to their different surface orientations. It was shown that when etching Si samples of different surface orientations (111) and (100), (100) faces show a larger concentration of kink sites that are more reactive (Allongue, et al., 1993). This could explain why the N_{crit}-value is greater for Cd deposition on n-Si(100) than it is in the case of n-Si(111).
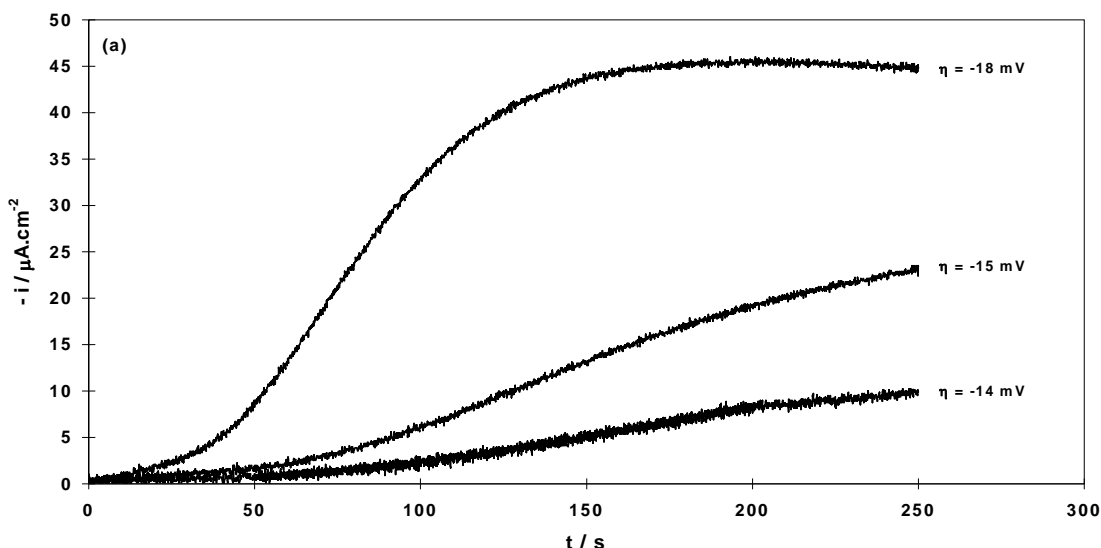

Figure 5a: Experimental current-time transients for Cd OPD at different overpotentials   in the system n-Si(111): 40-60 ohm.cm / 5 x 10^{-3} M $CdSO_4$ + 0.5 M Na_2SO_4 + 5 x 10^{-3} M H_2SO_4; pH = 2.5, T = 298 K. Initial potential $\Delta E_i = E - E_{Cd^{2+}/Cd} = 0$ mV.
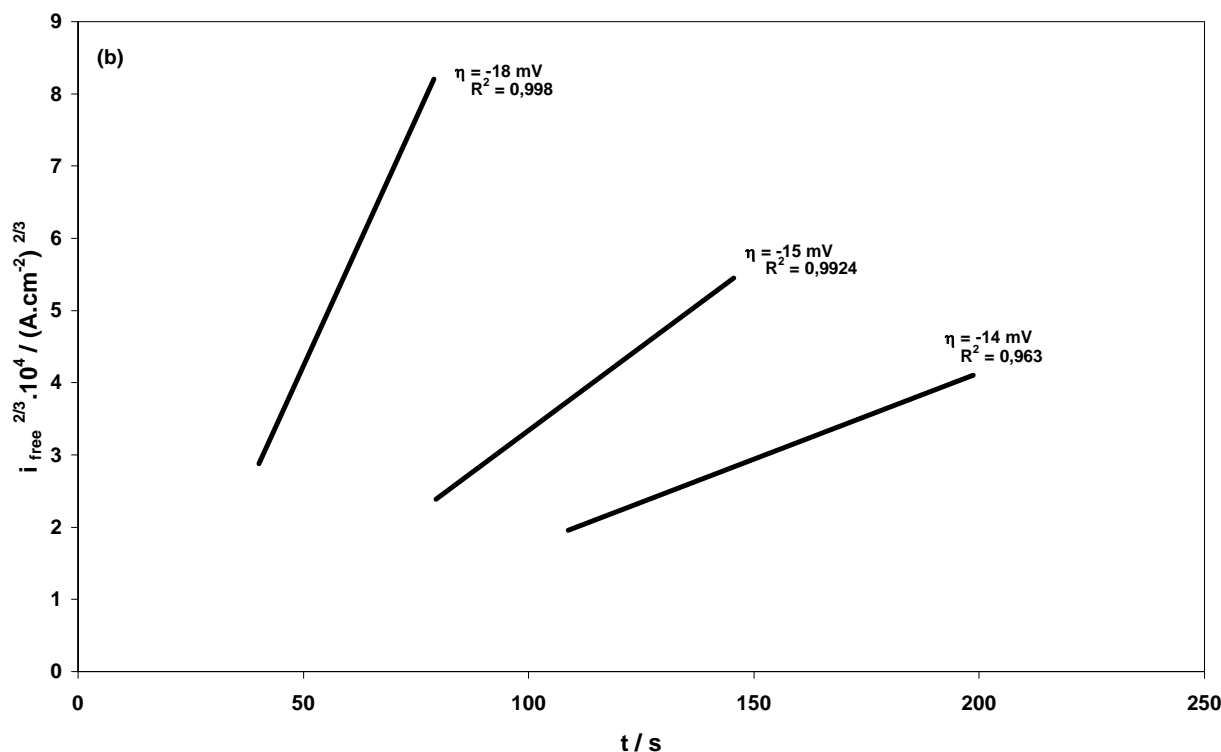

Figure 5b: $i_{free}^{2/3}$ vs. t plot of the initial parts of the transients shown in Figure 5a.

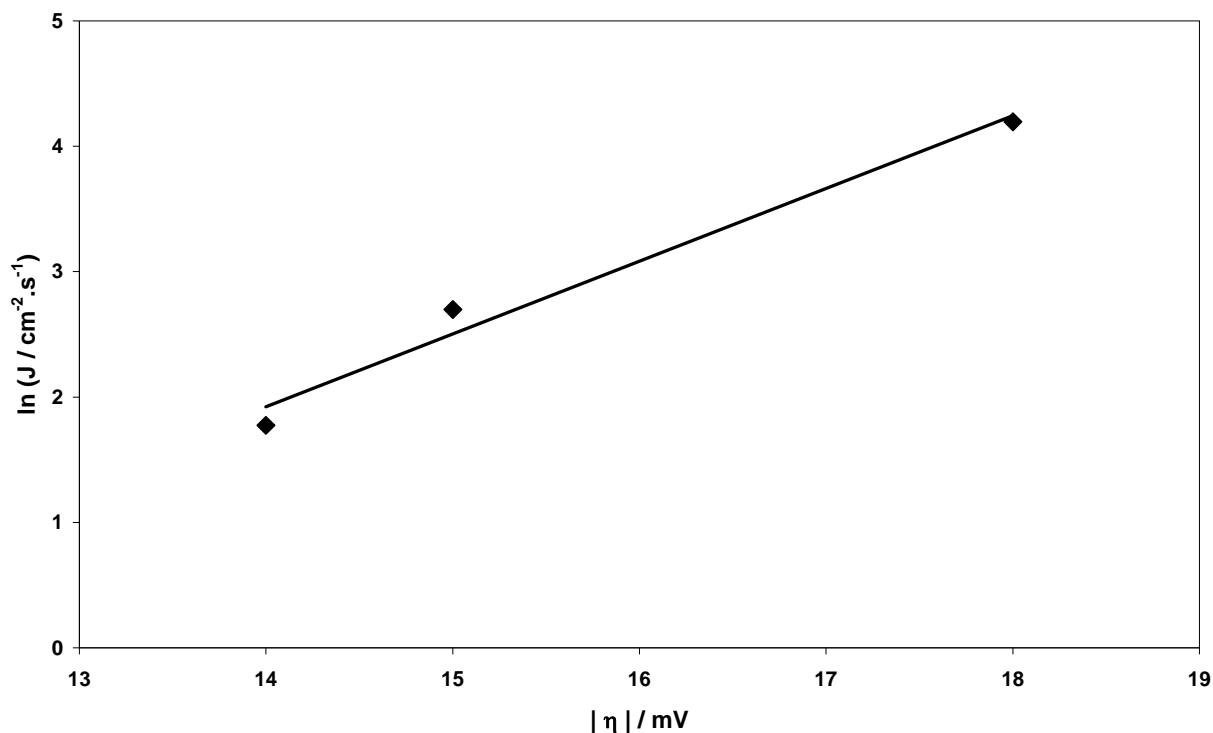Figure 6: Nucleation rate J as a function of the overpotential η. System n-Si(111): 40-60 ohm.cm / 5 x 10^{-3} M $CdSO_4$ + 0.5 M Na_2SO_4 + 5 x 10^{-3} M H_2SO_4; pH = 2.5, T = 298 K. Coefficient of determination of the straight line: R^2 = 0.9789. N_{crit} = 7 ± 1 atoms.

4. CONCLUSIONS

The initial Cd deposition kinetics on n-Si(100): 20-40 Ωcm resistivity and n-Si(111): 40-60 Ωcm resistivity can be described by a model involving progressive nucleation on active sites and hemispherical diffusion towards the growing 3D Cd clusters. Within the investigated overpotential range the number of atoms in the critical cluster was found to be N_{crit} = 16 ± 1 and N_{crit} = 7 ± 1 for n-Si(100) and n-Si(111) respectively. Such a difference in the N_{crit}-value can be related to the surface orientations of the silicon single crystals. The main factors determining the size of the critical nuclei and the Gibbs energy of nucleus formation are the supersaturation zF| η | and the Cd-Cd interaction on top of an unmodified Si substrate. In all cases the low values of N_{crit} indicate that the thermodynamics and kinetics of electrochemical nucleation must be described by the so-called small cluster or atomistic model (Budesvski, et al., 1996).

REFERENCES

Allongue, P., 1992. Physics and Applications of semiconductor Electrodes Covered with Metal Clusters. In Conway, B. I., Bockris, J. O'M., White, R. E.(Editors) Modern Aspects of Electrochemistry Vol. 23. Plenum Press, New York, pp.239-315.

Allongue, P., Costa-Kieling, V., Gerischer, H., 1993. Electrochemical Studies of n-Si(111) and (100) and Mechanism of the Dissolution. J. Electrochem. Soc. 140: 1018-1026.

Billo, E. Joseph, 1997. Excel for Chemists A Comprehensive Guide, WILEY-VCH, New York, 454 pages.

Bort, H., Jüttner, K., Lorenz, W. J., Staikov, G., 1983. Underpotential alloy formation in the system Ag(hkl)/Cd^{2+}. J. Electrochim. Acta 28 : 993-1001.

Brillsoin, L. J., 1982. The Structure and Properties of Metal-Semiconductor Interfaces. Surf. Sci. Report 2 : 123-326.

Budevski, E., Staikov, G. and Lorenz, W. J., 1996. Electrochemical Phase Formation and Growth- An Introduction to the Initial Stages of Metal Deposition, VCH, Weinheim, 410 pages.

Djenizian, T., Petite, B., Santinacci, L., Schmuki, P., 2001. Electron-beam induced carbon deposition used as a mask for cadmium sulfide deposition on Si(100). Electrochim. Acta 47: 891-897.

Golan, Y., Margulis, L., Hodes, G., Rubinstein, I., Hutchison, J. L., 1994. Electrodeposited quantum dots II. High-resolution electron microscopy of epitaxial CdSe nanocrystals on {111} gold. Surf. Sci. 311 : L633-L640.

Gómez, H., Henríquez, R., Schrebler, R., Riveros, G., Leinen, D., Ramos-Barrado, J.R., Dalchiele, E.A., 2004. A soft-solution electrochemical processing technique for preparing CdTe/n-Si(100) heterostructures. J. Electroanal. Chem. 574: 113-122.

Gómez, H., Henríquez, R., Schrebler, R., Córdova, R., Ramirez, D., Riveros, G., Dalchiele, E.A., 2005. Electrodeposition of CdTe thin films onto n-Si(100): nucleation and growth mechanisms. Electrochim. Acta 50 : 1299-1305.

Guel, B. 2007. Caractérisation structurale de diséléniures de métaux de transition et étude de quelques interfaces solide/électrolyte. Thesis, University of Ouagadougou, Burkina Faso, 252 pages.

Hodes, G., 1993. Size-Quantized Nanocristalline Semiconductors Films. Israel Journal of Chemistry 33: 95-106.

Hodes, G., Howell, I. D. J., Peter, L. M., 1992. Nanocristalline Photoelectrochemical Cells A New Concept in Photovoltaic Cells. J. Electrochem. Soc. 139(11): 3136-3140.

Hümann, S., Hommrich, J. and Wandelt, K., 2003. Underpotential deposition of cadmium on Cu (111) and Cu (100). Thin Solid Films 428: 76-82.

Khader, M. M. and Saleh, M. M., 1999. Comparative study between the photoelectrochemical behaviors of metal-loaded n- and p-GaAs. Thin Solid Films 349: 165-170.

Krumm, R., Guel, B., Schmitz, C. and Staikov, G., 2000. Nucleation and Growth in Electrodeposition of Metals on n-Si(111). Electrochim. Acta 45: 3255-3262.

Lobo, V. M. M., 1989. Handbook of Electrolyte Solutions Part A, Elsevier, Amsterdam, 300 pages.

Maupai, S., Zhang, Y. and Schmuki, P., 2003. Nanoscale obsevation of initial stages of Cd-electrodeposition on Au (111). Surface Science 527 : L165-L170.

Ortega, M., Santana, G., Morales-Acevedo, A., 2000. Optoelctronic properties of CdO/Si photodetectors. Solid-State Electronics 44: 1765-1769.

Pötzschke, R. T., Staikov, G., Lorenz, W. J., Wiesbeck, W., 1999. Electrochemical Nanostructuring of n-Si(111) Single Crystals Faces. J. Electrochem. Soc. 146 : 141-162.

Vidu, R. and Hara, S., 2000. Diffusion at Au(100)/Cd^{2+} interface during electrodeposition. Surface Science 452 : 229 -238.